Zbigniew GAWĘCKI
Roman NADOLSKI

CONSTRUCTION METHODS OF REDUCING COGGING TORQUE OF A DC BRUSHLESS MOTOR

ABSTRACT *The article presents selected construction methods for reducing the value of cogging torque at the design stage of DC brushless motors excited by permanent magnets. Calculations using the finite element method calculation (FEM) has been performed in Flux v.10.3 packet of Cedrat company. For the two prototype motors designs experimental studies have been performed.*

Keywords: *brushless dc motor, cogging torque, finite element method (FEM).*

1. INTRODUCTION

Brushless DC motors (called brushless direct current motors – BLDCM) in relation to "classical" DC motors have a better dynamic parameters, a higher power rate per unit volume, higher durability and lower maintenance costs [3, 11]. However, due to the design and method of BLDC motors phases supply, adverse electromagnetic torque ripple effects appear, which cause additional

Zbigniew GAWĘCKI, M.Sc.
e-mail: z.gawecki@tu.kielce.pl
Roman NADOLSKI, Prof.
e-mail: r.nadolski@tu.kielce.pl
Kielce University of Technology

power losses, vibration and noise [12]. One of the components of the electromagnetic torque is the cogging torque. It arises as a result of interaction of the rotor magnetic field (derived from permanent magnets) with the stator of angular variation of reluctance (uneven air gap) [7], which can be described by the relation:

$$T_{\mathrm{cog}}=-\frac{1}{2}\Phi^2\frac{\mathrm{d}R_{\mu}}{\mathrm{d}\theta_{\mathrm{m}}} \tag{1}$$

where:

Φ – magnetic flux in an air gap,
R_{μ} – air gap reluctance ,
θ_{m} – the angle of rotor rotation.

The issue of reducing cogging torque at the design stage of brushless motors is addressed in many works. The cogging torque can be reduced by:

- skewing stator slot [8, 12],
- application of magnets skew [4, 11],
- selection of the dimensions of magnets and air gap thickness [2, 3, 6],
- symmetrisation of air gap achieved by closing the stator slot by ferromagnetic wedge or by cutting stator's teeth [10],
- asymmetrical arrangement of magnets on the rotor [2, 9],
- immersing magnets in the rotor core [1, 2].

The most commonly applied and most effective are the first two of the above-mentioned methods.

This paper presents the results of simulation and experimental research involving two prototype constructions of brushless DC motor with an external rotor (so called upside-down construction). Considerations have been limited to the impact on the value of cogging torque of selected stator construction parameters and rotor that is skew slot, opening width of slot, height of air gap and the angle span of the magnets. The simulation research has been carried out, Flux 2D/3D environment, version 10.3 by Cedrat company using the finite element method (FEM) using quasi three-dimensional models ($2\,^1/_2$D) – FluxSkew module and three dimensional models – Flux3D module [5].

2. MOTOR CONSTRUCTION

The analysed motor has an inverted structure that is the rotating element is the exterior part, it allows gear-less drive through the cab of the engine directly in a driven element such as a circle, pump, fan etc. On the inside of the rotor are

attached high-energy permanent magnets made of rare earth elements such as neodymium-iron-boron. A simplified structure of the analysed motor is shown in Figure 1.

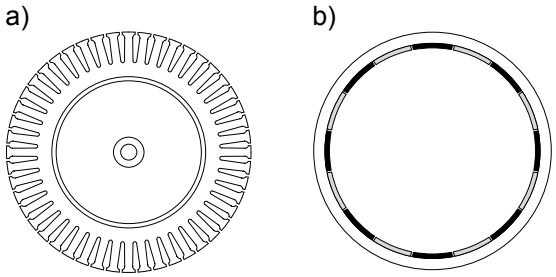

Fig. 1. Simplified construction of brushless DC motor:
a) a stator, b) rotor

The motor stator has been placed a three-phase winding which fragment has been shown in Figure 2. During normal operation, two of the three phases are powered, depending on the winding rotor position. Rotor position is identified by three Hall effect sensors, spaced by 120degE.

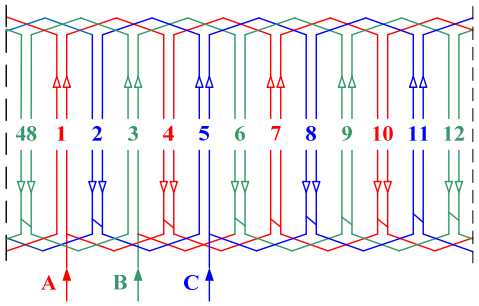

Fig. 2. Distributed diagram of winding fragment of a brushless motor

Selected electrical parameters and construction data presented in Table 1.

TABLE 1
Selected electrical parameters and construction data

Power supply	U_N = 24 V
Rated current	I_N = 8 A
Rated speed	n_N = 120 obr/min
Number of slots	N_s = 48
The number of slots per pole and phase	q = *1*
Number of phases	N_p = 3
Magnets material	$Nd_2Fe_{14}B$
Magnets height	h_m = 3 mm
Coercivity	H_c = 900 kA/m
Remanence	B_r = 1.2 T
Energy density	(BH_{max}) = 270 kJ/m^3
Number of rotor poles	p_r = 16

3. SIMULATION MOTOR MODELS

During field calculations non-linearity of magnetic motor circuit has been taken into account and the following simplifying assumptions have been taken into consideration [3, 9]:

- discussions have been limited to the magneto-static field,
- coil windings were replaced by rails leading current,
- constant current density has been adopted throughout the rails cross--section,
- omission of the phenomenon of inducing eddy currents in the motor stator due the low speed of rotor,
- adopted a zero normal component of magnetic induction at the sufficiently distant edge from an analysed object.

Taking into account the rotational symmetry of the analysed structure, the calculation area was limited to the total, that is to τ_S pole pitch (Figures 3a, 3b and Figure 4).

a) b)

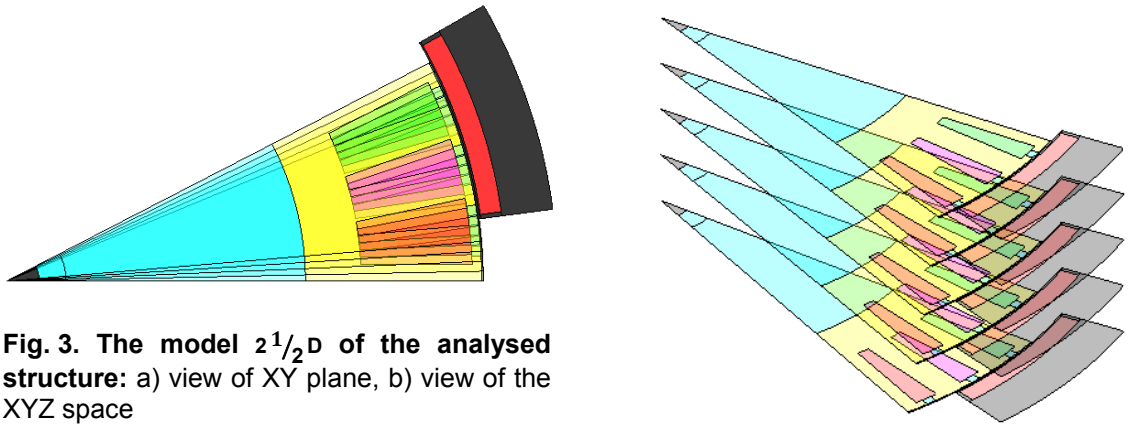

Fig. 3. The model $2\frac{1}{2}$D of the analysed structure: a) view of XY plane, b) view of the XYZ space

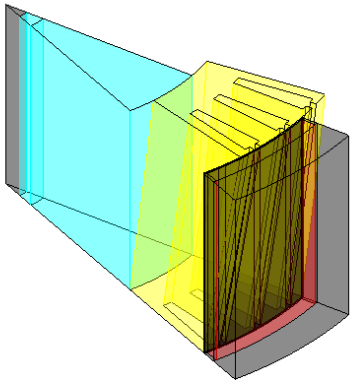

Fig. 4. The model 3D of the analysed structure

A multi-layered model shown in Figure 3 was built using FluxSkew module using ,,Multilayers 2D'' method [5]. The angle of stator skew slot α_s has been included by dividing the machine to l_a active length a certain number of layers N_L. Each layer represents $1/l_a$ the engine length, the last layer is rotated by a defined angle of rotation α_s, and intermediate layers are rotated by $N_{La}*(\alpha_s/N_L)$ angle, N_{la} – current layer number. The number of layers, declared at the beginning of the simulation, affects the accuracy and calculation time. Increasing the number of layers increases the accuracy of the calculations, however, causing the prolongation of the simulation. In the analysed case the number of layers has been set at $N_L = 5$, since increasing the number of layers did not significantly improve the results of calculations.

For typical stator stack angles 0 deg, 7.5 deg, 15 deg calculation tests have been performed in 3D space using "Extruded 3D"method and Flux3D module [5]. Three-dimensional model is created by "impression" of flat primer in the third dimension and the division of a model for a certain number of elements along the active length of the machine.

4. RESULTS OF CALCULATIONS

Coggingtorque was determined by internal functions of Flux2D/3D package as a derivative of W' magnetic coenergy changes relative to the angle of rotation of the rotor θ_m [5, 11]:

$$T_{cog}(\theta_m) = -\frac{\partial W'}{\partial \theta_m} \tag{2}$$

The calculations of cogging torque were carried out within the slot pitch for the current in stator windings $I = 0$, the electromagnetic torque calculations were performed for rated current $I = 8$ A changing the position of the rotor every 0.25degM (which corresponds to 2degE).

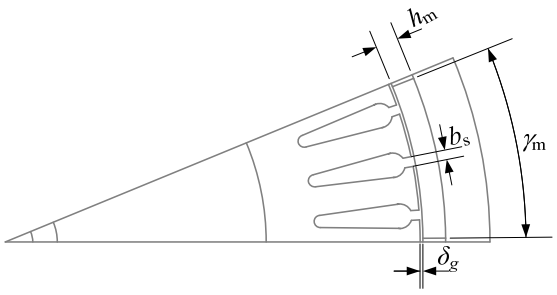

Fig. 5. BLDC motor pole pitch:
h_m – magnet height,
b_s – slot opening width,
δ_g – air gap height,
γ_m – angular magnet spread

Figure 6 shows the dependence of T_c cogging torque of the stator slot skew angle in an electro-less state.

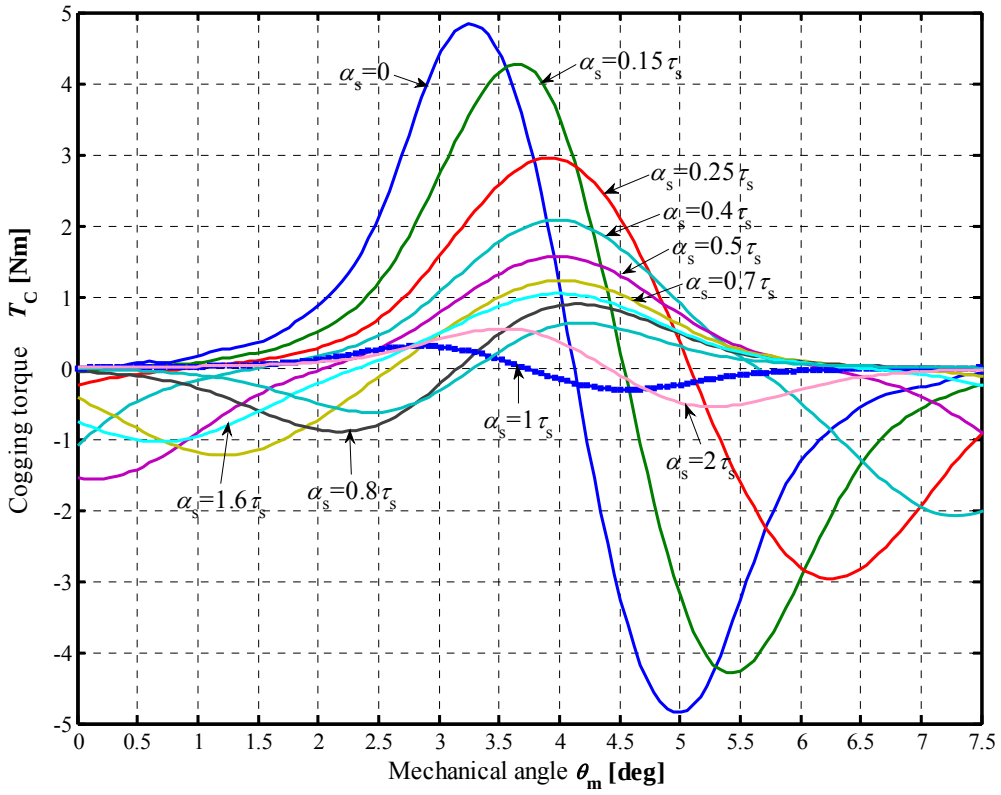

Fig. 6. The dependence of T_c cogging torque from θ_m rotor position angle for certain angles skew of stator slot α_s

As follows from carried out calculations the smallest amplitude of cogging torque T_{cmax} = 0.331 Nm for the analysed structure (prototype A) can be obtained for the angle of the stator slot skew 7.5 deg, while for the output construction (prototype B) the amplitude of cogging torque T_{cmax} = = 0.611 Nm (Fig. 7). For slot stator skew angles which 0 deg, 7.5 deg, 15 deg have been performed using a three--dimensional model. Figure 7 shows comparison dependences for slot stator skew angles 7.5 deg with quasi three-dimensional and three-dimensional calculations.

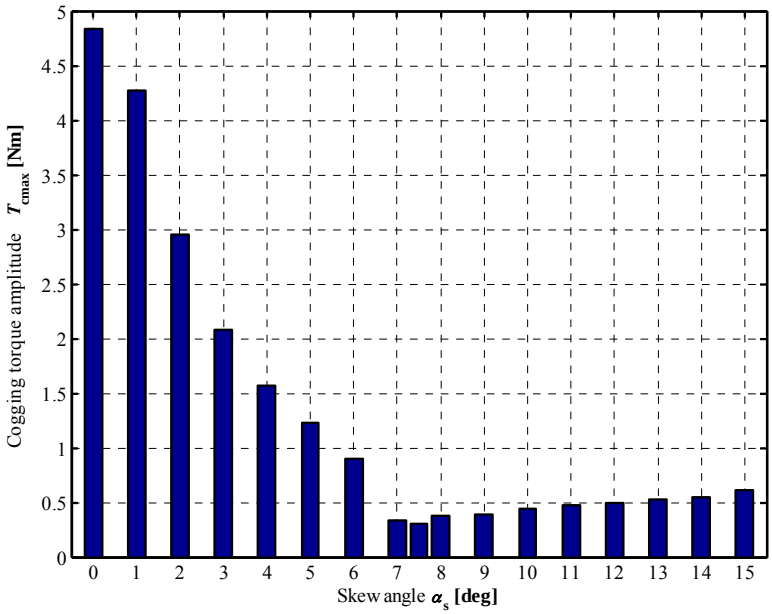

Fig. 7. Dependence of cogging torque amplitude T_{cmax} from stator stack angle α_S

Amplitudes in both cases are comparable, while the difference in shape is due to simplification of the method $2\,^1/_2$ D [5].

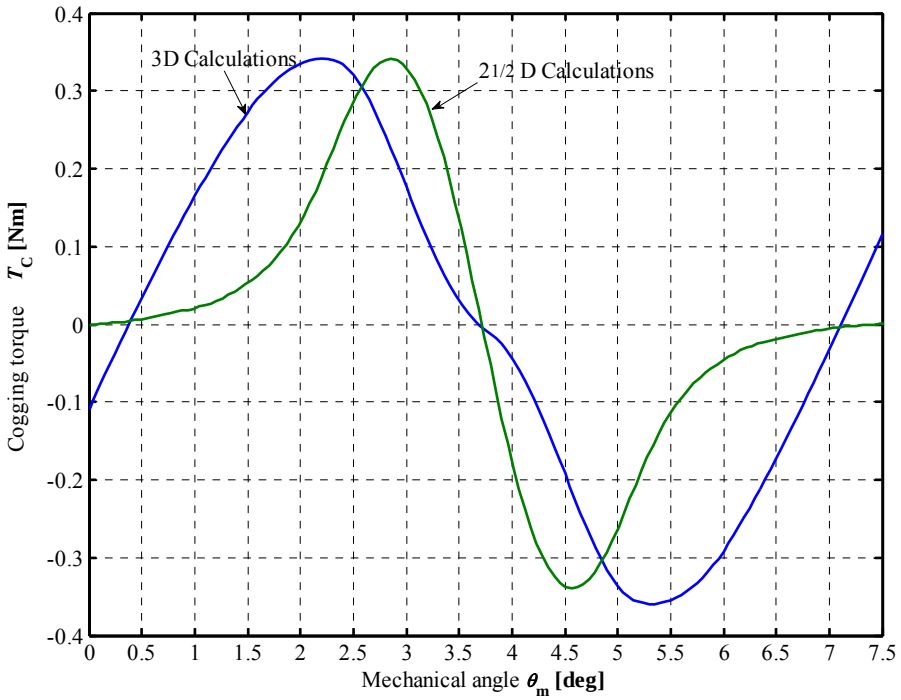

Fig. 8. The dependence of T_c cogging torque form rotor position angle θ_m for the stator slot skew angle α_s = 7.5 deg

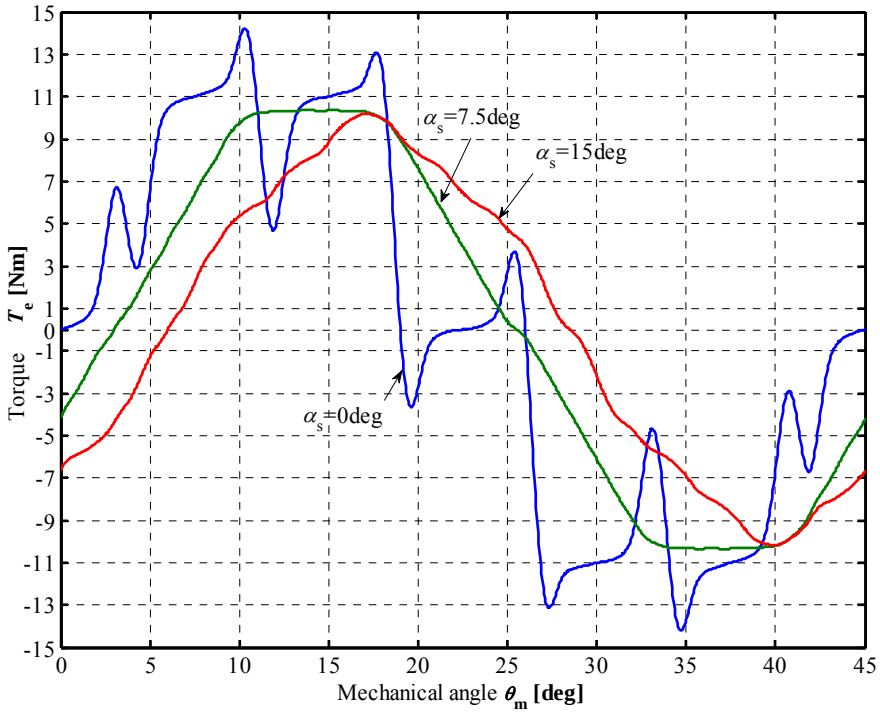

Fig. 9. The dependence of the electromagnetic torque T_e on the rotor position angle θ_m for stator stack angles α_s = 0; 7.5; 15 deg when running two phases winding

For stator slot skew angles ranging 0 deg, 7.5 deg, 15 deg also performed calculations of an electromagnetic torque at a current in two phases I = 8 A (Fig. 9). As in other works [11, 12] on the issue of reducing cogging torque, percentage coefficient of the content of cogging torque in the electromagnetic torque has been defined:

$$\tau = \frac{T_{\text{cmax}}}{T_{\text{max}}} * 100\% \tag{3}$$

where:

T_{cmax} – the maximum value of cogging torque,

T_{max} – the maximum value of electromagnetic torque.

For slot stator skew angles ranging 0 deg, 7.5 deg, 15 deg; τ coefficient is respectively 33.9%, 3.18%, 6.01%. Selection of the appropriate a slot stator skew angle allows for significant reduction of impact of cogging torque on the shape and value of the electromagnetic torque.

In Figure 10 shows the effect of γ_{mr} magnet angular spread referred to the pole pitch τ_{p} at a constant height of the air gap and magnet on cogging torque.

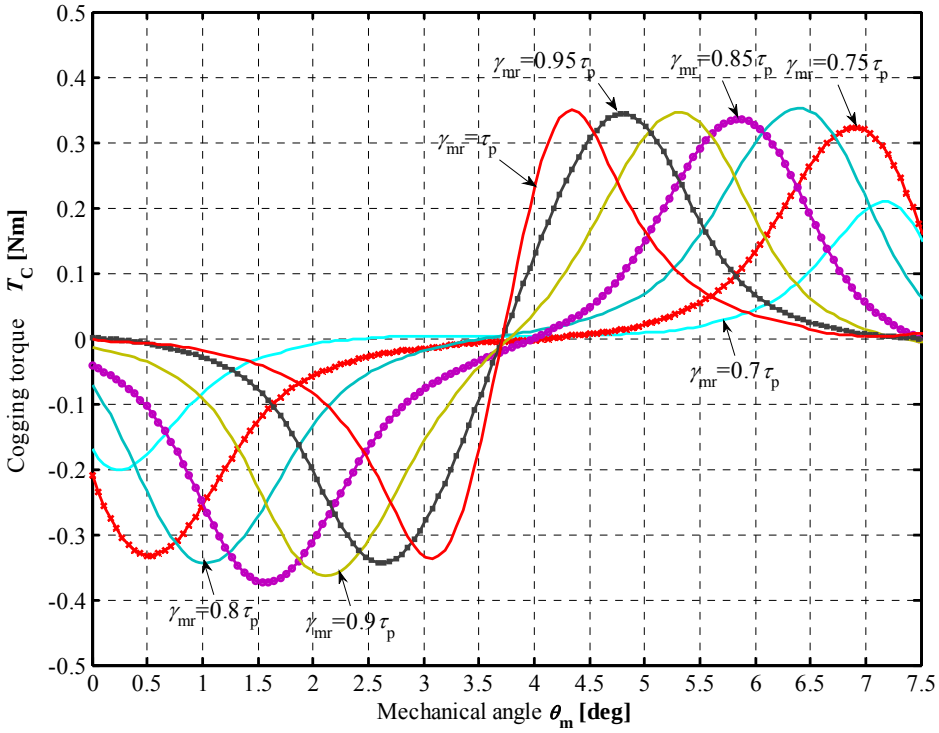

Fig. 10. Dependence of T_c cogging torque from magnet angular range γ_{mr}

Magnet angle range slightly affects the amplitude of cogging torque, but has a significant influence on the electromagnetic torque.

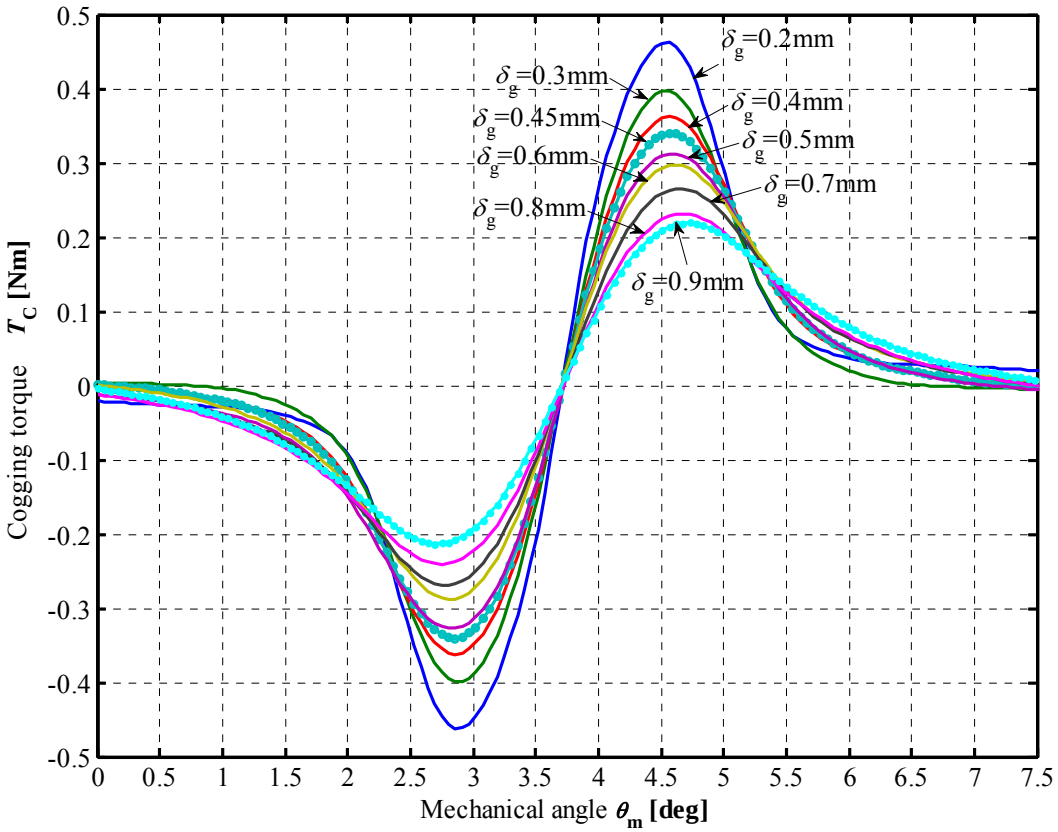

Fig. 11. Dependence of T_c cogging torque from the height of the air gap δ_g

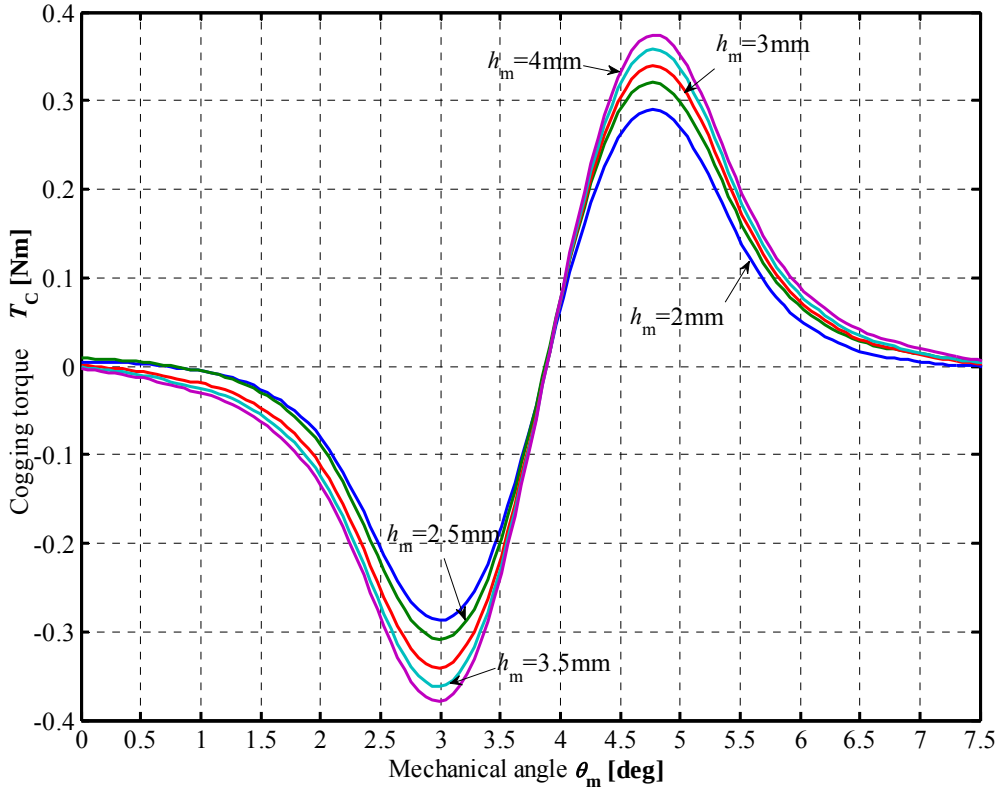

Fig. 12. Dependence of T_c cogging torque from the magnet height h_m

The impact of the air gap height δ_g and the magnet height h_m for permanent magnet angular range onto cogging torque has been shown in Figure 11 and 12. However, during the construction calculations, selection of an appropriate height of air gap and the magnet does not result from the necessity to minimize cogging torque, but the selection of a suitable operating point of the magnet [3, 7].

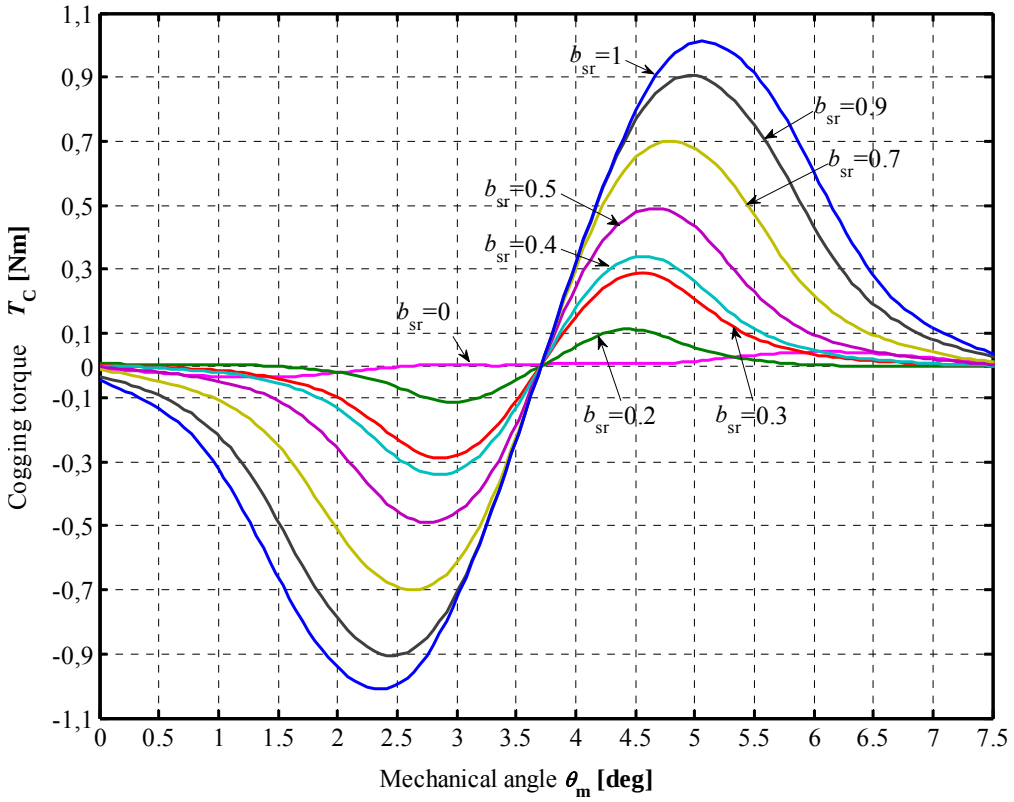

Fig. 13. Dependence of T_c cogging torque from the relative slot opening b_{sr}

Figure 13 shows the effect of b_{sr} slot opening referenced to the slot pitch τ_s on cogging torque. The minimum value of the cogging torque can be obtained for the complete closure of a slot b_{sr} = 0, thanks to which one obtains uniform air gap. The necessity to wind the stator with a wire of a certain diameter makes that is the analysed construction b_{sr} = 0.4.

In order to verify the simulation calculations were carried out research on prototypes A and B which were analysed at the stand equipped, among others, in T32FNA contactless transducer for measuring torque and rotational speed of Hottinger Baldwin Messtechnik company and cooperating with it MGCPlus measuring amplifier. The research was conducted at low rotation in electro-less state propelling the motors. Recorded waveforms (Fig. 14a and 14b) show that stator slot skew corresponding to one slot pitch allows for reduction of cogging torque by almost a half.

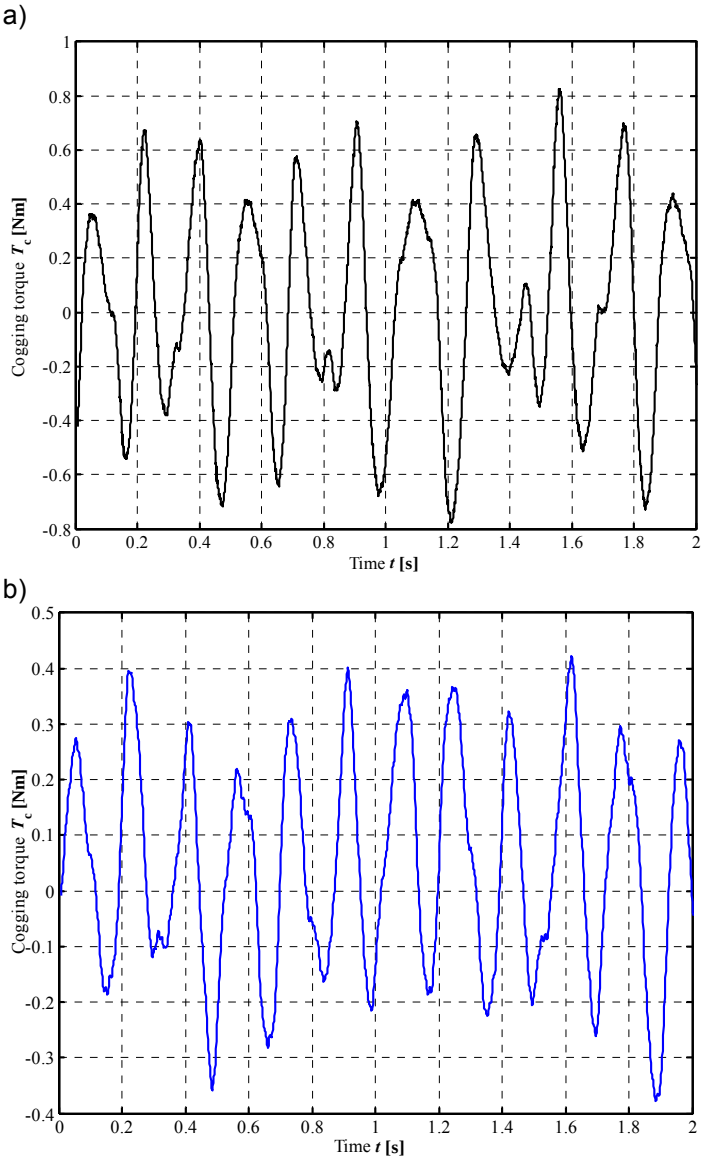

Fig. 14. Registered time waveforms of T_c cogging torque: a) the prototype B – skew angle of 15 deg, b) the prototype A – skew angle of 7.5 deg

5. SUMMARY

The paper analyses the impact of selected construction parameters on the value of cogging torque in a brushless motor with external rotor. $2\,^1/_2$D and 3D models were used in numerical calculations. Due to time-consuming calculations using three-dimensional models, most calculations have been performed using a quasi-three-dimensional models. Application of a proper stator slot skew has allowed for nearly 50% reduction of cogging torque. In addition, construction of 7.5 deg stator slot skew has a much more advantageous shape of the electromagnetic torque which translates into higher effi-

ciency. The correctness of simulations were verified by experimental research of two prototype constructions of brushless motors. Recorded research results confirmed the reduction of cogging torque, which was the aim of this work.

The work was co-funded by the Ministry of Science and Higher Education under a promotion grant No. N N510 332337.

LITERATURE

1. Aydin M., Ronghai Q., Lipo T.A.: Cogging torque minimization technique for multiple-rotor, axial-flux, surface-mounted-PM motors: alternating magnet pole-arcs in facing rotors, 38th Industry Applications Conference, IAS Annual Meeting, USA, Salt Lake City 2003, vol. 1, pp. 555-561.
2. Aydin M.: Magnet skew in cogging torque minimization of axial gap permanent magnet motors, ICEM'2008, 6-9 September, Vilamoure, Portugal, 2008, Paper ID 1186.
3. Ciurys M., Dudzikowski I.: Analiza wpływu wymiarów i kształtu magnesów trwałych na moment elektromagnetyczny bezszczotkowego silnika prądu stałego, Prace Naukowe Instytutu Maszyn, Napędów i Pomiarów Elektrycznych Politechniki Wrocławskiej, Nr 58, Studia i Materiały, Nr 25, Wrocław, 2005.
4. Dosiek L., Pillay P.: Cogging torque reduction in permanent magnet machines, IEEE Transactions on Industry Application, Vol. 43, No. 6, November/December 2007, p. 1565-1571.
5. Flux ver.10.3 – Documentation and Examples, Cedrat.
6. Garcia P.M., Guemes J.A., Moreno V., Iraolagoitia A.M.: Influence of constructive parameters on the cogging torque in PMSMs, 11th Spanish-Portuquese Conference on Electrical Machines, Zaragoza, 1-4 July, 2009.
7. Hanselman D.: Brushless permanent magnet motor design, Second Edition, The Writers' Collective, Cranston, Rhode Island, 2003.
8. Hanselman D.C.: Effect of skew, pole count and slot count on brushless motor radial force, cogging torque and back EMF, IEE Proceedings Electric Power Applications, September 1997, vol. 144, no. 5, pp. 325-330.
9. Keyhani A., Sebastian T.: Study of cogging torque in permanent magnet machines, IEEE IAS Annual Meeting, USA, New Orleans, Louisiana, 1997, pp. 42-49.
10. Kim K., Sim D., Won J.: Analysis of skew effects on cogging torque and BEMF for BLDCM, IEEE IAS 1991, 26th Annual Meeting Industrial Applications Society, USA, Dearborn 1991, vol. 1, pp. 191-197.
11. Korkosz M., Młot A.: Analiza pulsacji momentu elektromagnetycznego w bezszczotkowym silniku prądu stałego z zastosowaniem skośnych magnesów, BOBRME-KOMEL, Zeszyty Problemowe-Maszyny Elektryczne, Nr 88, Katowice, 2010, s. 47-51.
12. Młot A., Łukaniszyn M., Korkosz M.: Wpływ skosu stojana na redukcję pulsacji momentu elektromagnetycznego w bezszczotkowym silniku prądu stałego, BOBRME-KOMEL, Zeszyty Problemowe-Maszyny Elektryczne, Nr 88, Katowice, 2010, s. 41-45.

Manuscript submitted 12.12.2011

METODY KONSTRUKCYJNE ZMNIEJSZANIA MOMENTU ZACZEPOWEGO W SILNIKU BEZSZCZOTKOWYM PRĄDU STAŁEGO

Zbigniew GAWĘCKI, Roman NADOLSKI

STRESZCZENIE *W pracy przedstawiono wyniki badań symulacyjnych i eksperymentalnych dotyczących silników bezszczotkowych z zewnętrznym wirnikiem (budowa odwrócona). Przeprowadzono analizę wpływu wybranych wymiarów geometrycznych na wartość momentu zaczepowego i pulsacje momentu elektromagnetycznego.*
Silniki bezszczotkowe wzbudzane magnesami trwałymi z pierwiastków z ziem rzadkich w ostatnich latach znajdują coraz szersze obszary zastosowania, m.in. bezprzekładniowy napęd lekkich pojazdów zasilanych z baterii akumulatorów. Jednym z problemów, którym zajmuje się wiele zespołów badawczych [1-12], jest zmniejszenie wartości momentu zaczepowego już na etapie projektowania silnika. Moment zaczepowy powstaje w wyniku współdziałania pola magnetycznego wirnika (pochodzącego od magnesów trwałych) ze stojanem o kątowej zmienności reluktancji (nierównomierna szczelina powietrzna). Moment zaczepowy jest niekorzystną składową wypadkowego momentu elektromagnetycznego, która wywołuje pulsacje, drgania, hałas i dodatkowe straty mocy. Obliczenia momentu zaczepowego na etapie projektowania można wykonać, wykorzystując np. metodę elementów skończonych w specjalizowanych środowiskach, takich jak Flux firmy Cedrat.

W pracy przeanalizowano wpływ skosu żłóbków, szerokości otwarcia żłobków, wysokości szczeliny powietrznej, wysokości i rozpiętości kątowej magnesów na moment zaczepowy i elektromagnetyczny. Badania symulacyjne zrealizowano w środowisku Flux wersja 10.3 przy użyciu modeli quasi-trójwymiarowych ($2^1/_2 D$) i modeli trójwymiarowych (3D). Na podstawie wyników obliczeń wybrano i fizycznie zrealizowano rozwiązanie konstrukcyjne charakteryzujące się najmniejszą wartością momentu zaczepowego i najkorzystniejszym przebiegiem momentu elektromagnetycznego. Przeprowadzone badania eksperymentalne potwierdziły zmniejszenie wartości momentu zaczepowego i zmniejszenie pulsacji wypadkowego momentu elektromagnetycznego.